Chapter 3. Alignment procedure for the convergent optical correlator

Once we have obtained the optimal configuration of the SLMs to use them in amplitude only regime or phase only regime we proceed to build the real time correlator.

3.1. Elements that require alignment

The VanderLugt correlator described in Chapter 1 permits to perform frequency filtering operations, including correlation for optical pattern recognition. However, to operate appropriately it is necessary to have a correct matching between the Fourier spectrum of the input image, obtained by light diffraction, and the filter, which is digitally introduced onto the filter SLM.

So, it is necessary to control those aspects that are involved in such a correspondence. They are (see Figure 3.1):

a) The focusing of the Fourier spectrum of the scene onto the filter SLM.

b) The centering of the filter SLM onto the optical axis, which is the center of the optically obtained spectrum of the input scene.

c) The azimuth angles of the filter SLM and of the scene SLM so as to have parallelism between the coordinate axes of the spectrum of the scene and the filter.

d) The scaling of the Fourier spectrum obtained at the filter plane, so as to control not only the direction but also the magnitude of the frequencies that are filtered.

We propose in this Chapter a series of tests that allow us to control these parameters. The proposed tests are original and satisfy the following conditions:

a) They are based on the interpretation of the image at the correlation plane. This way there is no need to use additional control devices in the correlator.

b) The tests have a simple interpretation. So, one can relate the observed pattern to the frequency filtering operation that is performed in the filter plane.

c) The tests are sensitive to only one of the parameters that must be controlled. That is, they produce an identifiable response to a given misalignment of the system careless of the other misalignments of the system.

d) It results convenient to have a sequential alignment procedure. That is to control each parameter without affecting the others. In other case a recursive procedure, much slower, can be used. The procedure must take into account that some parameters must be controlled before the rest of tests can be used. As an example, let us consider the case of the filter focusing, one can not talk about frequency filtering if the Fourier spectrum of the scene is not focused on the filter plane.

e) Finally, the filtering tests take into account two possibilities of operation for the scene SLM: the amplitude only regime, and the phase only regime. For the filter SLM we consider phase only modulation because along this thesis we will use phase only filters.

Aside from the spectrum focusing test, which has an interferometric interpretation, the tests proposed in this chapter are based on phase frequency filtering. For each parameter to be aligned, we design an input scene that generates a frequency spectrum distribution that is differently affected by a filter when only one of the alignment parameters changes.

Because we want a simple interpretation of the filtered patterns, we use periodic gratings, that generate discrete spectra and we see how binary filters applied to them affect the reconstruction of the gratings.

3.2. Description of the correlator and sequence of the alignment procedure.

We consider the convergent set up of the Vander Lugt correlator. It is a variant of the Vander Lugt correlator in which the distance between the scene and the filter fixes the scale of the Fourier transform of the scene.

3.2.1. *Description of the correlator*

We represent the scheme of a convergent correlator in Figure 3.1.

A previous description of the correlator has been given in Chapter 1 and we repeat in this section a more detailed description. The beam at 458 nm generated by an Ar^+ ion laser is focused on a pinhole by a microscope objective. The pinhole (s) is the light source for the correlator. The image of the pinhole is focused by a lens (L_1) on s'. Instead of a singlet lens, we use a 135 mm focal distance photographic objective, corrected off-axis and for spherical aberrations.

The input image (scene), is represented in the spatial light modulator marked as SLM_1. in Figure 3.1. It is illuminated by the spherical wave that converges in s'. The Fraunhofer diffraction pattern of the scene represented in SLM_1 is obtained at the plane that contains s'. (we refer to this plane as S'). The amplitude distribution at S', noted $a_{S'}(x,y)$, is the Fourier spectrum of the amplitude distribution at the input scene,

multiplied by a quadratic phase factor **[Moreno96B]**, as follows:

$$a_{S'}(x,y) = C\exp\left[i\frac{\pi}{\lambda D}\left(x^2+y^2\right)\right]F\left(\frac{x}{\lambda D},\frac{y}{\lambda D}\right). \qquad (3.1)$$

Here C is a normalization constant and D represents the distance between the input SLM and the plane S' (see Figure 3.1). $F(x,y)$ represents the Fourier spectrum of the amplitude distribution at the output of SLM_1. Note that the scale of the Fourier spectrum of the scene depends on D, and therefore it can be controlled by changing the position of SLM_1 along the optical axis of the correlator.

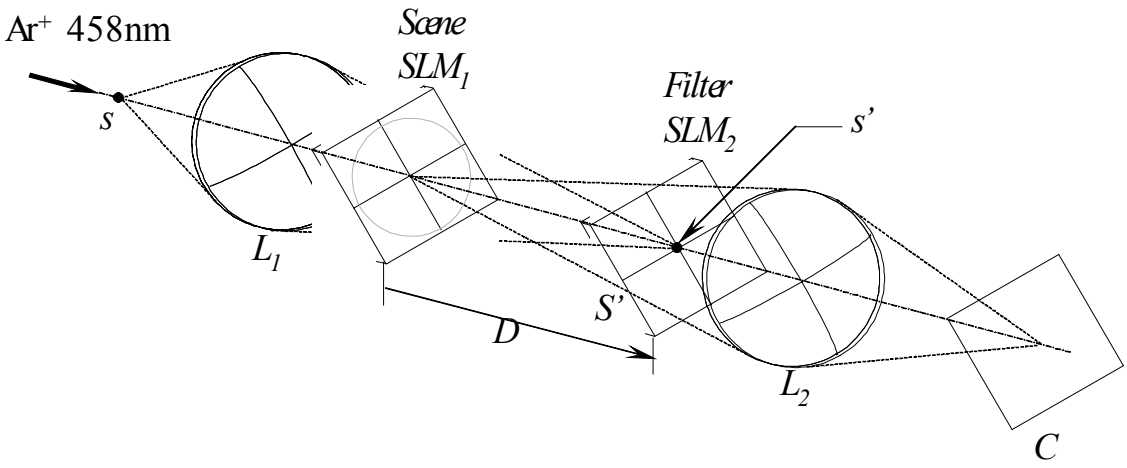

Figure 3.1. Scheme of the convergent correlator.

The filter SLM (marked as SLM_2 in Figure 3.1) is placed at the plane S', where the frequency spectrum of the scene is focused. This way, one knows S' as the filter plane. The transmittance or the phase modulation distribution of the filter SLM multiplies the frequency spectrum of the input scene. The filtered image of

the scene is focused on the correlation plane *C* by the second lens of the correlator (L_2). We acquire the correlation plane by placing on *C* the CCD array of a Pulnix TM-765 camera, connected to a PC computer provided with real time acquisition software.

3.2.2. *Sequence of the alignment procedure*

To perform the alignment of the correlator it is necessary to adjust several elements. Aside from the lenses, that must be correctly tilted and centered on the optical axis, one needs to adjust the position of the scene and the filter SLMs, and the position of the CCD camera used to acquire the correlation plane.

To move one of the elements of the correlator in order to adjust a given alignment parameter may introduce a misalignment on the other parameters. Therefore it is necessary to establish a sequence of the alignment to avoid this trouble. We describe next the sequence we propose.

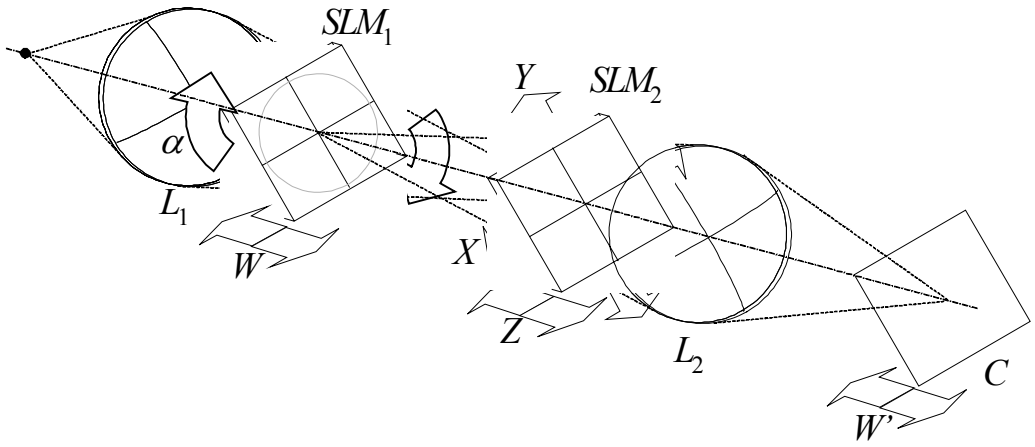

Figure 3.2. Scheme of the convergent correlator with arrows that indicate the movements needed to perform the alignment.

The first step is to focus the input scene on the correlation plane *C* (Figure 3.2) by shifting the camera along the optical axis, this movement is tabbed as *W'* in Figure 3.2. This step is necessary because the tests are based on the observation of the correlation plane. To do this it is enough to focus the scene when SLM_2 does not display any filter.

Then, one performs the test for focusing the scene spectrum on the filter plane. This can be done by shifting SLM_2 along the optical axis. We represent this movement by the arrow tabbed as *Z* in Figure 3.2.

The next step is to center the filter SLM (SLM_2) on the optical axis (the arrows *X* and *Y* in Figure 3.2). Therefore it is necessary to mount the filter SLM on a translation stage that allows to move on these orthogonal directions. (See picture in Figure 3.3a)

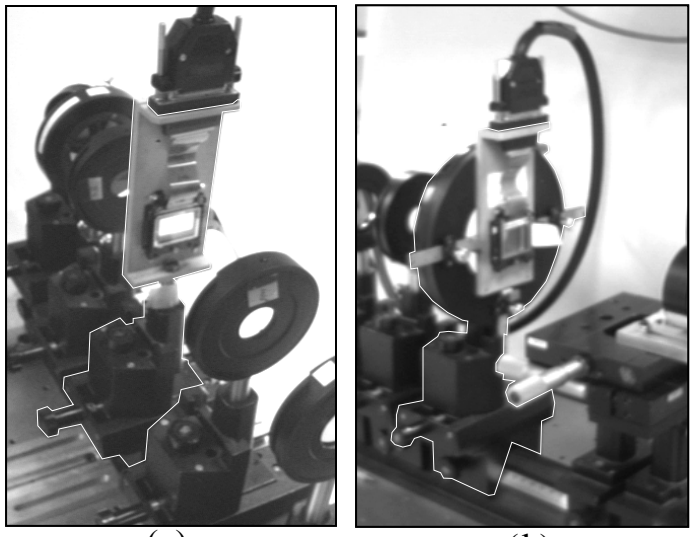

Figure 3.3. (a) Filter SLM mounted on a *XY* translation stage on a *Z* translation rail (b) Scene SLM mounted on a rotation stage on the same translation rail as the filter SLM.

Then we propose to perform the azimuth alignment by rotating the scene SLM (SLM_1) instead of rotating the filter SLM (SLM_2). This way, one avoids to move the center of the pixel array of the filter SLM out of the optical axis when the rotation center of the mount of the filter panel is not the same as the center of the pixel array. We represent this movement by the arrow tabbed as α in Figure 3.2. Figure 3.3b shows a picture of the rotation stage used for the scene SLM we have used in our correlator.

Finally, we propose to fit the scale of the scene spectrum and the filter by translating the input scene SLM along the optical axis (represented by the arrow tabbed *W* in Figure 3.2). Even in the case that the translation stage shifts the scene modulator transversally, this translation does not affect the centering or the orientation of the diffraction pattern in the filter plane.

Therefore it does not alter the previous alignment steps of the proposed procedure. Nevertheless, to change the position of the scene must be accompanied of a refocusing of the correlation plane, that is, it is necessary to translate the CCD camera along the optical axis of the system (see the arrow *W'* in Figure 3.2).

In the following sections we describe the tests that we have invented for the alignment of the correlator and the results we have obtained.

3.3. Fine focusing of the scene spectrum on the filter plane

The test we propose to focus the scene spectrum on the filter plane is an interferometric test in which SLM_2 is used to alter the wavefront that propagates from the pinhole along the correlator. At this stage of the alignment procedure one cannot talk precisely about frequency filtering because the Fourier spectrum of the scene is not well focused on SLM_2 yet.

The test we propose to perform this step of the alignment of the correlator consists of displaying a uniform image in the scene SLM (SLM_1) with maximum transmission, and displaying a π radian phase line in SLM_2 Figure 3.4a is a representation of the test filter. The phase profile is shown in Figure 3.4b.

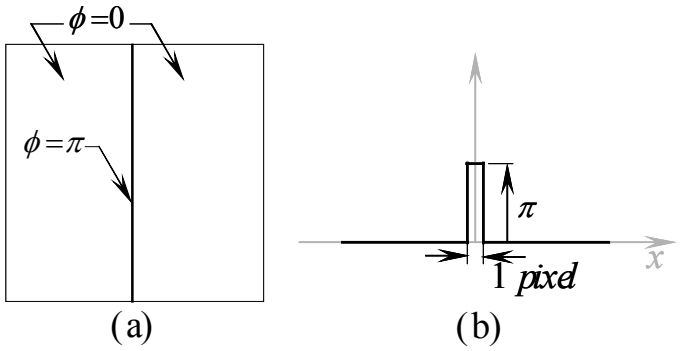

Figure 3.4. (a) Filter for filter-focusing test. (b) Profile representation of the phase for the filter.

Because the transmission and phase modulation of the scene SLM is uniform, the light that comes from the pinhole is distributed as a spherical wave that converges on *s'* till the plane where the filter SLM is placed. There, this spherical wave is filtered by the test filter. The test filter is represented by the following function $H(x,y)$:

$$H(x,y)=1+\delta(x)(e^{i\pi}-1)=1-2\delta(x), \qquad (3.2)$$

where δ is the Kronecker function. The two terms of the filter correspond to the uniform background and the π phase line for the pixels on the x=0 axis. Both terms multiply the spherical wavefront at the filter input. Therefore, the amplitude distribution at the output side of SLM_2 is given by:

$$A_{SLM2}(x,y)=\frac{A_0}{\lambda d}\exp i2\pi\frac{d}{\lambda}\exp i\pi\frac{y^2}{\lambda d}\left[\exp i\pi\frac{x^2}{\lambda d}-2\delta(x)\right], \qquad (3.3)$$

Here A_0 is a normalization factor, λ is the wavelength of the light and d is the distance from SLM_2 to the pinhole image, *s'*.

Taking this into account, one can consider that two wavefronts come out from the filter: the first one corresponds to the spherical wave that propagates from the pinhole along the optical system without distortion, and the second one is a wavefront generated by the phase line in SLM_2. These two wavefronts produce an interference pattern observable on the correlation plane. In addition, because this interference pattern depends on the distance d from the filter SLM to s' it may be used to perform the focusing of the scene spectrum on SLM_2.

From equation 3.3 one can deduce that the dependence on the variable y for both wavefronts is identical. That is, the filter distribution only introduces differences in the amplitude distribution of the waves along the x direction.

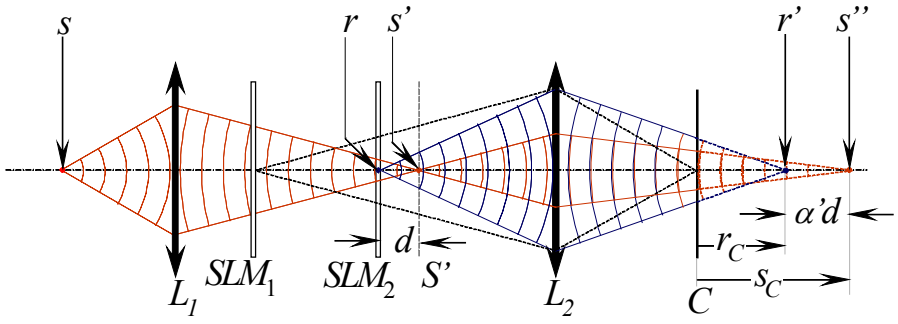

Figure 3.5. Representation of the correlator and the wavefronts that produce the interference pattern in the correlation plane for the filter-focusing-test.

Regarding only at the x distribution of the wavefronts (equations 3.3), one observes that the first term describes a wavefront that converges on s'. This is represented Figure 3.5, colored in red. After passing through L_2, this wavefront

converges on *s”*, that is the image of the pinhole through L_1 and L_2.

The second wavefront, however, is generated at SLM_2 (colored in blue in Figure 3.5), therefore after passing through L_2 it converges on the image plane through L_2 of the filter SLM, noted as *r’*. This way, at the correlation plane *C* the amplitude distribution (considering only the x dimension) is given by:

$$A(x) = A_C\left[\exp i\pi\frac{x^2}{\lambda s_C} - 2\exp i\pi\frac{x^2}{\lambda r_C}\right], \qquad (3.4)$$

Where s_C and r_C are the distances from the correlation plane to *s”* and *r’* respectively.

Therefore the intensity distribution in the correlation plane is given by:

$$I(x) = I_C\left[5 - 4\cos\pi\frac{(r_C - s_C)x^2}{\lambda s_C r_C}\right]. \qquad (3.5)$$

That is, it describes a fringe pattern depending on x^2 that depends directly on the distance between *r’* and *s”* (Figure 3.5), and therefore on the distance *d* between SLM_2 and *s’* through the axial magnification relation $r_C - s_C = \alpha' d$ (see Figure 3.5).

According to equation 3.5 some fringes appear in the correlation plane. These fringes are wider as smaller *d* is, and when the filter is placed on *s’*, that is, for $d=0$, the fringes

become infinitely wide, and a uniform field is observed in the correlation plane.

In Figure 3.6 we show the experimental captures of the correlation plane for different positions of the filter SLM when the filter focusing test is being performed. Figure 3.6a and b show captures of the correlation plane when the filter SLM is far from focus (in Figure 3.6a it is farther than in Figure 3.6b). One can observe a fringe pattern depending on x^2. The fringes become wider when the position of the filter SLM approaches image plane of the pinhole. This is represented in Figure 3.6b and c, where one can observe that the fringes are wider. Finally, when the filter SLM is exactly on the image plane of the pinhole, the fringes disappear, as shown in Figure 3.6d.

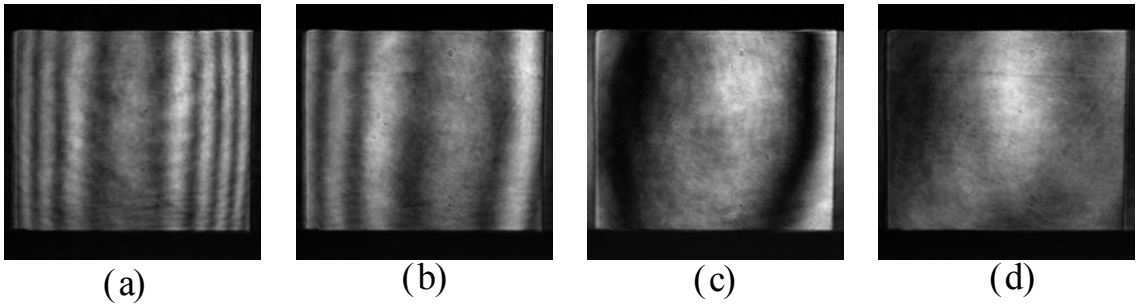

Figure 3.6. Experimental captures of the intensity distribution in the correlation plane for the filter focusing test. (a) and (b) Far from focus (c) near to focus. (d) on focus.

This way, the focusing procedure consists of shifting SLM_2 along the optical axis and observing in which direction the fringes of the correlation plane become wider. The focusing position is achieved when the fringes observed in the correlation plane become a uniform image.

Note that this test is suitable for either amplitude-encoded or phase-encoded scene correlators because a constant function is displayed in the input SLM (SLM_1).

3.4. Centering of the filter for amplitude only scene

Once the Fourier spectrum of the input scene is correctly focused over the filter plane the center of the filter SLM must be moved transversally so as to place the center over the optical axis, which is where the center of the scene Fourier spectrum is.

This alignment is performed in two steps, first the filter is aligned horizontally, and then it is aligned vertically. To control both the horizontal position and the vertical position we use the same alignment test, but for the vertical centering the tests are rotated by 90 degrees with respect to the horizontal centering test.

3.4.1. *The test scene and filter*

The scene and filter corresponding to this test are shown in Figure 3.7a and b respectively. The scene consists on a series of binary gratings along the x direction, with even symmetry. The lower frequency is $1/N_x$ periods per pixel, being N_x the size in pixels along the x direction. This frequency corresponds to the grating at the bottom of the image. The frequencies for the other gratings, from bottom upwards are obtained by doubling the frequency of the previous grating.

The filter we propose for this test (shown in Figure 3.7b) consists of a centered vertical line of one pixel width, in which the phase difference to the background is π. It is the same filter as for the filter focusing test. When one of the diffraction orders of the gratings of the scene coincides with the phase line, its phase is changed by an amount of π radians, or what is the same, its sign is inverted.

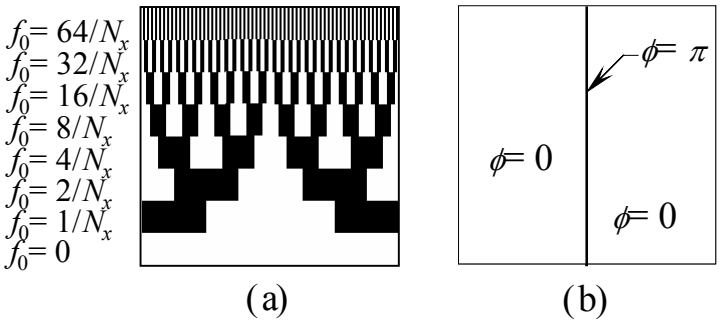

Figure 3.7. Horizontal centering test scene (a) and filter (b).

The amplitude transmission for each grating is given by.

$$t(x) = \frac{A_{\max}}{2}\left(1 + \operatorname{sgn}\cos 2\pi \frac{x}{x_0}\right), \tag{3.6}$$

where $A_{\max}$ is the high value of the amplitude grating, and x_0 is the period of the grating, and it is equal to $1/f_0$. We also use the *sign* function, defined as follows:

$$\operatorname{sgn} a = \begin{cases} -1 \ \ if \ a < 0 \\ +1 \ \ if \ a \geq 0 \end{cases}, \tag{3.7}$$

Because the considered gratings have even symmetry and have period x_0, they can be written as the contribution of a series of

cosine gratings with frequencies multiple of the fundamental frequency ($f_0=1/x_0$), this is represented in Figure 3.8. The binary grating in Figure 3.8a is decomposed as the addition of the cosine grating series in Figure 3.8b. This decomposition can be expressed as follows.

$$d(x)=\sum_{n=0}^{\infty} A(n)\cos 2\pi\frac{nx}{x_0}, \qquad (3.8)$$

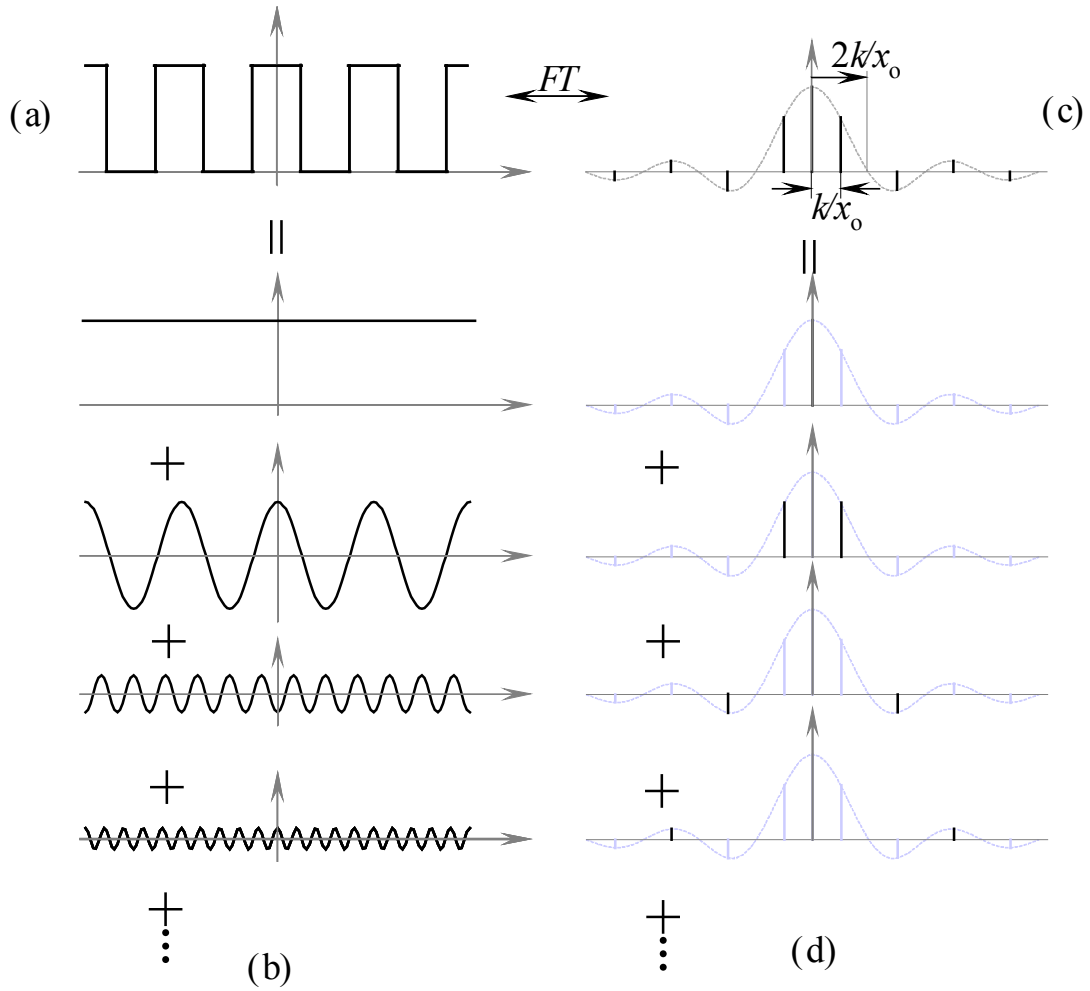

Figure 3.8. (a) Binary cosine grating. (b) The grating can be considered as the contribution of a series of cosine gratings. (c) Corresponding Fourier spectrum. (d) The Fourier spectrum of the binary grating is also a series of spectra corresponding to the cosine gratings.

$A(n)$ is the amplitude of the n-th order of the discrete Fourier spectrum of the grating. To obtain these terms we consider the binary grating as the convolution of a *comb* function of period x_0 with a *window* function, constant between $-x_0/4$ and $+x_0/4$, and null elsewhere. Therefore the Fourier spectrum of the binary grating is the product of the Fourier spectrum of the *comb* function by the Fourier spectrum of the window function. This is represented in Figure 3.8c. There, one can observe the discrete diffraction orders, spaced by a distance of k/x_0, being k a proportionality constant. This corresponds to the *comb* function. The peaks are modulated by the *sinc* function corresponding to the Fourier spectrum of the window function. And it has the first minimum at a distance $2k/x_0$ from the origin.

The Fourier spectrum in Figure 3.8c can also be decomposed in terms of the spectra of the series of cosine gratings. This is represented in Figure 3.8d. This way, the DC peak corresponds to the average value of the grating, and each couple of peaks at the same distance from the origin represent the two linear phases that generate the cosine function terms.

The *sinc* function that modulates the Fourier spectrum peaks determines the amplitude of each one of the terms in the series. This amplitude is given by:

$$A(n) = A_{\max} \frac{2}{n\pi} \sin\frac{n\pi}{2}, \qquad (3.9)$$

Because in the test scene there are gratings with different periods, the Fourier spectrum of the whole scene presents the peaks for the different gratings (see Figure 3.9). For each one of the binary gratings there is the DC order, the fundamental orders and also the harmonic orders. We represent in Figure 3.9b the correspondence between the peaks of the Fourier spectrum and four different gratings of the scene in Figure 3.9a. The spectrum of the whole image (see Figure 3.9c) is the superposition of the spectra for each one of the gratings, as represented in Figure 3.9d. The gratings with higher period have their fundamental orders closer to the origin, while the gratings with small period have the fundamental orders far from the origin. Of course the DC for all the gratings is at the center of the spectrum. In the correlator that is at the intersection of the filter plane with the optical axis.

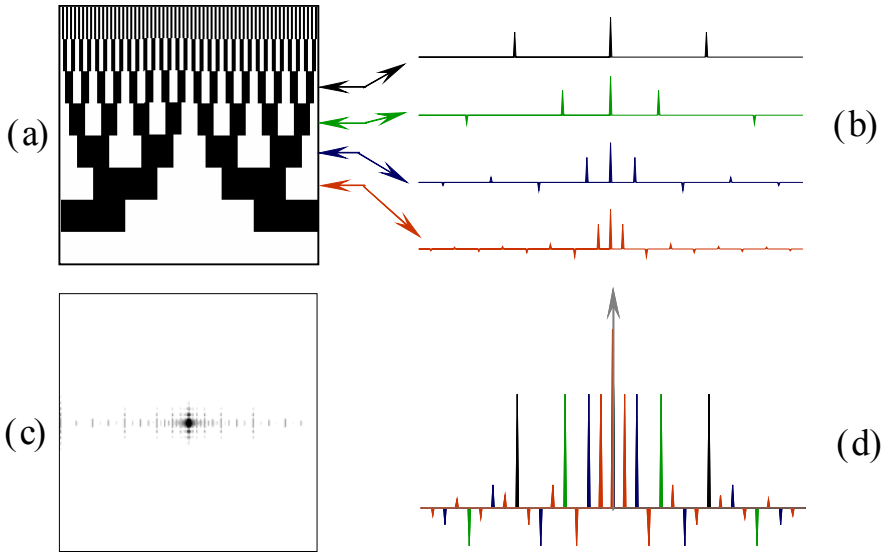

Figure 3.9. Spectrum of the test scene. (a) test scene and (b) the peaks corresponding to the different gratings. (c) Squared magnitude of the Fourier spectrum of the scene. (d) Profile of the real part of the spectrum. It results from the contribution of the peaks for all the gratings.

This way, the test scene generates a correspondence of the different points along the *x* axis of the Fourier spectrum with the image of the gratings reconstructed in the correlation plane. When the filter inverts the sign of a peak far from the origin it alters a high frequency grating, and when it inverts a peak close to the origin it alters a low frequency grating. In addition, because all the gratings have the DC at the origin of the Fourier spectrum, when the filter affects the center of the Fourier spectrum all the gratings are affected.

Let us analyze in detail how the reconstruction of the test scene gratings is affected when the different diffraction orders are inverted.

3.4.2. *Binary grating filtering*

Because the filter is a single vertical line of one pixel width, it inverts only one of the orders of the Fourier spectrum of a grating. As explained in section 3.4.1, each couple of diffraction orders on the Fourier spectrum of a grating at opposite distances from the origin constitute one of the cosine terms in the series given in equation 3.8. Because the inverse Fourier transform of each peak corresponds to a linear phase term one can retrieve that they contribute to the amplitude distribution at the correlation plane following the well known relation:

$$\cos 2\pi \frac{x}{x_0} = \frac{1}{2}\left[\exp\left(+i2\pi \frac{x}{x_0}\right) + \exp\left(-i2\pi \frac{x}{x_0}\right)\right] \qquad (3.10)$$

This way, when one adds a π radians phase to one of the peaks, one inverts the sign of one of these linear phase terms. Therefore the mentioned filtering operation, noted $\mathbf{H}_{(+k/xo)}[]$, applied to a cosine function produces the following result:

$$H_{+1}\left[\cos 2\pi \frac{x}{x_0}\right] = \frac{1}{2}\left[-\exp\left(+i2\pi \frac{x}{x_0}\right) + \exp\left(-i2\pi \frac{x}{x_0}\right)\right] = i\sin 2\pi \frac{x}{x_0} \qquad (3.11)$$

That is, the real-valued cosine grating is changed by an imaginary valued sine grating.

This same interpretation can be extended for the binary grating. When one of the peaks, corresponding to the harmonic orders of the binary grating are changed, one of the cosine terms of the series becomes an imaginary sine term. That is expressed as follows:

$$d(x) = \frac{A_{\max}}{2}\left(1 + \operatorname{sgn}\cos 2\pi \frac{x}{x_0}\right) - A(n)\cos 2\pi \frac{nx}{x_0} + iA(n)\sin 2\pi \frac{nx}{x_0}, \qquad (3.12)$$

And the corresponding intensity at the correlation plane is:

$$I_n(x) = A^2(n) + \frac{1}{2}\left(1 + \operatorname{sgn}\cos 2\pi \frac{x}{x_0}\right)\left(A^2{}_{\max} - 2A_{\max}A(n)\cos 2\pi \frac{nx}{x_0}\right), \qquad (3.13)$$

And replacing the explicit expression of $A(n)$ given in 3.9 we obtain

$$I_n(x) = I_{\max}\left[\left(\frac{4}{n\pi}\sin\frac{n\pi}{2}\right)^2 + \frac{1}{2}\left(1+\operatorname{sgn}\cos 2\pi\frac{x}{x_0}\right)\left(1-\frac{4}{n\pi}\sin\frac{n\pi}{2}\cos 2\pi\frac{nx}{x_0}\right)\right] \quad (3.14)$$

Here $I_{max} = A_{max}^2$. The intensity distribution of the reconstructed grating, after being filtered depends on the diffraction order affected by the grating. We represent in Figure 3.10a the intensity distribution at the correlation plane for the cases in which there is no filtering, and when the inverted order is n=1, 3 and 5. Figure 3.10b is a representation of the intensity dependency on the x direction at the corresponding Fourier plane. And Figure 3.10c represents the filtered Fourier spectrum of the grating. One can observe that there is a notable difference between the unfiltered reconstruction and the reconstruction when the fundamental order (n=1) is altered. Because the energy of the higher order harmonics is very low, to affect them does not produce a very important change.

A special filtering case is when the inverted order is the DC. In this case the altered term of the Fourier series is not a term of a cosine component but the constant average value. The reconstructed grating in this case can be obtained by subtracting to the original amplitude distribution the double of its average value. This way one writes:

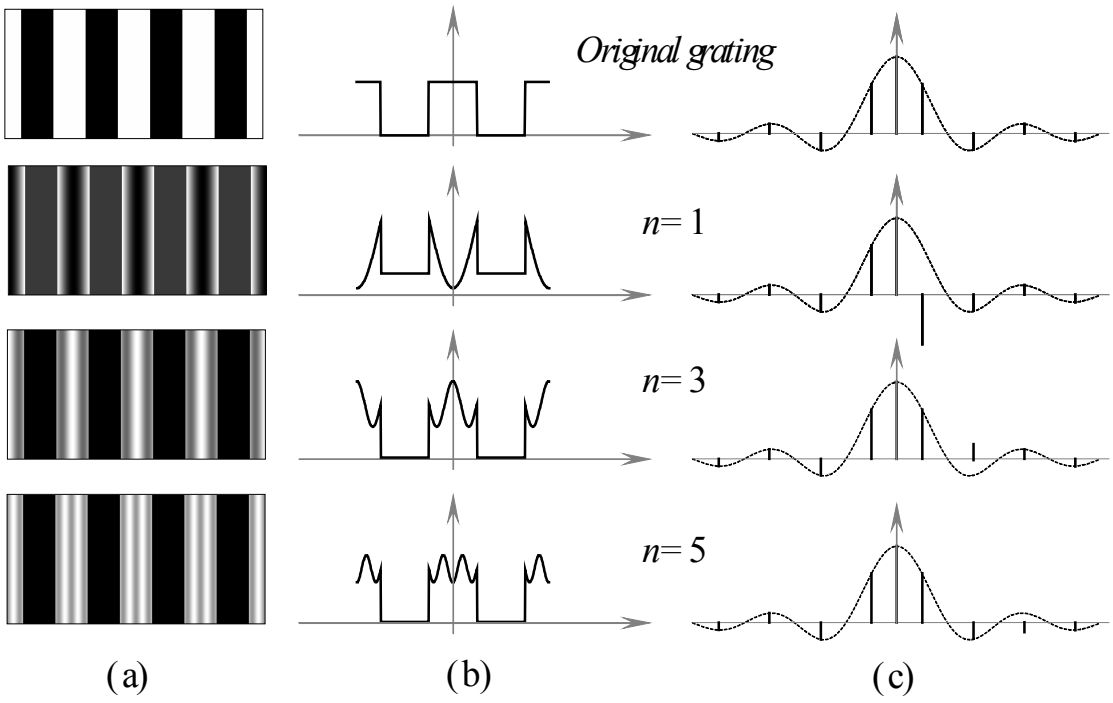

Figure 3.10. Reconstruction of the grating binary grating after the inversion of the harmonic terms of order n=1,3 and 5. (a) Image reconstruction. (b) Intensity profile (c) Corresponding real part of the Fourier spectrum.

$$H_0[a(x)] = \frac{A_{\max}}{2}\left(1+\operatorname{sgncos}2\pi\frac{x}{x_0}\right) - 2\frac{1}{x_0}\int_0^{x_0}\frac{A_{\max}}{2}\left(1+\operatorname{sgncos}2\pi\frac{x}{x_0}\right)dx, \quad (3.15)$$
$$= -\frac{A_{\max}}{2}\left(1-\operatorname{sgncos}2\pi\frac{x}{x_0}\right)$$

and the corresponding intensity distribution at the correlation plane is given by:

$$I_0(x) = \frac{I_{\max}}{2}\left(1-\operatorname{sgncos}2\pi\frac{x}{x_0}\right), \quad (3.16)$$

That is the resulting intensity distribution, represented in Figure 3.11a, is a binary grating complementary to the original grating (represented in Figure 3.11b). That is, the inversion of

the DC order produces a contrast inversion of the original grating.

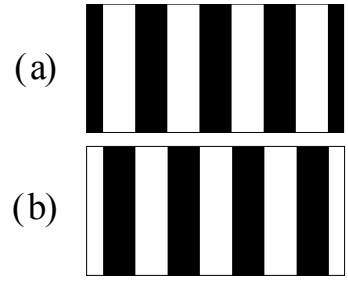

Figure 3.11. Reconstruction of a binary grating when the sign of the DC term is inverted (a) reconstructed grating. (b) original grating.

Because the DC peak for any grating is placed on the origin of the spectrum, the contrast of all the gratings in the test scene are inverted at the same time when the phase line crosses the optical axis of the correlator.

Therefore, the observation of the reconstruction of the test scene on correlation plane when the test filter is applied can be used to center the filter SLM on the optical axis. Next we detail the procedure.

3.4.3. *The centering procedure*

By shifting the SLM along the x direction, one may place the phase line of the SLM over one of the fundamental orders of a grating, this can be clearly observed at the correlation plane. If the affected grating has period $N_x/2^n$ measured in pixels, then the x=0 axis of the SLM is placed at $M2^n$ pixels of the optical axis. Here M is the scale factor between the filter and the Fourier spectrum of the scene, which is not still matched at this

stage of the alignment procedure. For any value of *M*, when the filter SLM gets closer to the centered position, the period of the affected grating is bigger. Finally, when the x=0 axis of the filter SLM crosses the optical axis, one observes the contrast inversion of all the gratings of the test scene.

We show in Figure 3.12 experimental results for the centering procedure performed onto our convergent optical correlator. Figure 3.12a is the image of the test scene at the correlation plane, when there is no filter. In this case, all the gratings are well reconstructed.

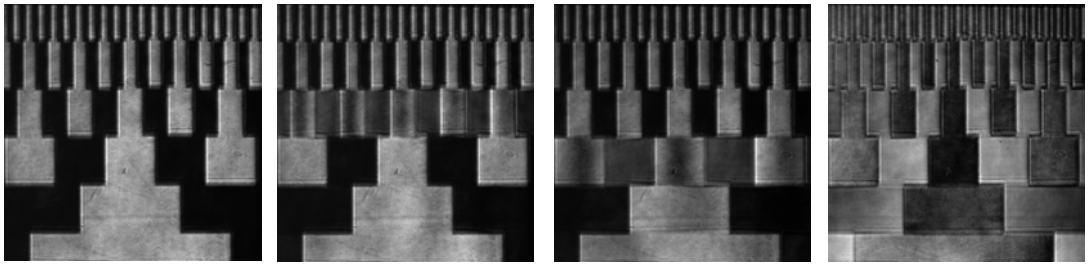

(a) (b) (c) (d)

Figure 3.12. Test for the horizontal centering of the Filter SLM (a) Unfiltered image of the test scene. (b) Image for a misalignment of 320 μm. (c) Image for a misalignment of 160μm. (d) image for the correct centering

Figure 3.12b shows a case in which the fundamental order of the grating with period $N_x/8$ is inverted, and therefore the distortion predicted by equation 3.14 is observed in the image. One can deduce that the x=0 axis of the filter SLM is at $8=2^3$

pixels from the origin of the scene Fourier spectrum[†]. That is, considering that the distance between pixels of the filter SLM used in the correlator is 40 μm, one deduces that the filter is misaligned horizontally by about 320 μm. The image in Figure 3.12c shows the case when the x=0 axis of the filter SLM is at about 160μm of the center of the scene Fourier spectrum. So, the grating with period $N_x/4$ is distorted. Finally, the case when the filter SLM is horizontally centered on the optical axis is shown in Figure 3.12d. In this case the DC term of all the gratings in the scene are inverted, and a contrast inversion of the scene is observed. Because the filter phase line has a width of one pixel the accuracy of the centering process is one pixel, that is 40 μm.

3.4.4. *Vertical centering considerations*

Once the filter is horizontally centered, the same test, with the scene and filter rotated 90 degrees, is used to center the filter SLM vertically. We show in Figure 3.13 the captures of the correlation plane for different positions of the filter. In Figure 3.13a, b and c the filter is misaligned by 32, 16 and 8 pixels respectively. We show the reconstruction of the scene when the filter is vertically aligned in Figure 3.13d.

[†] Considering that the scaling factor between the scene Fourier spectrum and the filter SLM is M=1

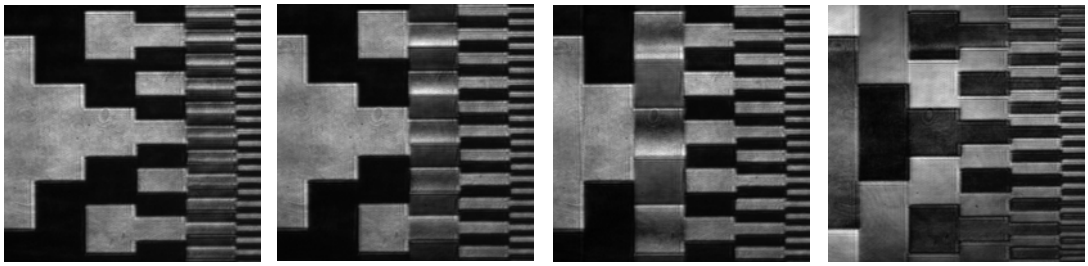

Figure 3.13. Captures of the correlation plane for the vertical alignment test. The corresponding misalignment amounts are: (a) 32 pixels, (b) 16 pixels, (c) 8 pixels. (d) Contrast inversion produced for the correct vertical centering.

Sometimes, depending on the mount of the filter SLM, the shift axes (S_x and S_y in Figure 3.14) are not exactly parallel to the SLM pixel array axes (x and y in Figure 3.14). In this case, the centering process must be an iterative process. This is because the test is designed to detect when the x or y axes of the filter intersect with the center of the scene Fourier spectrum. This way, when the centering of the x axis of the filter is performed and the filter is moved along the S_x axis, the position of the y axis is changed (because the component of S_x along the y axis is nonzero). Therefore the y axis must be re-aligned. We represent this in Figure 3.14. We show the case in which the shift directions of the SLM mount (S_x,S_y) and the axes of the pixel array (x,y) are not parallel. We represent with arrows the trajectories on the SLM of the Fourier spectrum center when the centering procedure is performed.

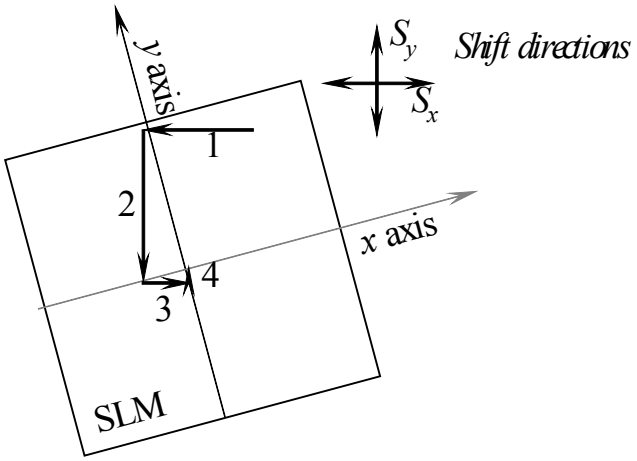

Figure 3.14. Trajectory of the center of the scene Fourier spectrum when the centering procedure is applied to a filter SLM with the shift directions (S_x,S_y) different to the pixel array axes (x,y).

The horizontal centering procedure brings the origin of the scene Fourier spectrum to the y axis (see the arrow marked as 1 in Figure 3.14), however the vertical centering (arrow 2) moves it out. However, if the deviation between the shift axes and the filter SLM axes is less than 45 degrees the iterative process converges towards the centered position (see arrows 3 and 4). Usually, the angle between the shift directions and the x, y axes of the pixel array is very small, so the process converges fast.

3.4.5. *Additional verifications*

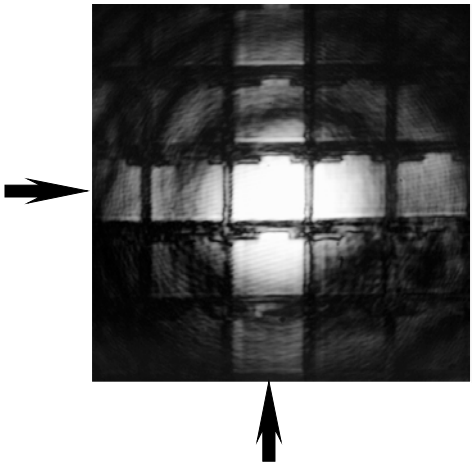

Figure 3.15. Image of the pinhole at s', acquired by using a microscope objective placed behind the filter SLM. The arrows show the one pixel cross sent to the origin of the SLM.

A direct verification of the filter focusing test and the filter centering test is shown in Figure 3.15. It consists of the image of the center of the filter SLM, magnified using a microscope objective, when a uniform scene is displayed in the input SLM. A centered cross is displayed in the filter SLM. The cross is composed by vertical and a horizontal line of one pixel width. In addition, because the filter SLM is configured in phase only regime we have changed the polarization configuration behind the modulator so as to make the cross visible. One can observe that the pinhole image (an Airy disk) and the pixel array are well focused at the same plane. This shows that the filter is correctly placed on the image plane of the source, and therefore the input scene spectrum is well focused on the filter SLM.

One can also observe that the center of the Airy disk is placed inside the center of the cross, that is on the center of the modulator. That means that the filter is correctly centered on the optical axis of the correlator.

3.5. Alignment of the scene azimuth to the filter.

The next step in the alignment procedure described in Section 3.2.2 is the azimuth matching of the scene and the filter SLMs. One must consider that one of the SLMs of the correlator may be slightly rotated about the optical axis with respect to the other SLM. In this case the axes determined by the pixel array of the scene modulator, and the axes of the filter SLM are not exactly parallel each other. Therefore, according to Section 3.2.2 the azimuth (α in Figure 3.2) of the scene modulator must be matched to the azimuth of the filter SLM.

3.5.1. *The test scene and filter*

The test we propose for the azimuth matching step of the alignment procedure of the correlator consists on displaying the test scene shown in Figure 3.16a and the filter shown in Figure 3.16b. The proposed scene consists of a series of wedges in all the directions separated by 5 degrees each other. We refer to this as a wedge star. Instead of the horizontal wedges, we have represented a thin line (one pixel width) in the x direction. We consider this line as a reference line. Because it is thinner than the wedges it provides better accuracy in the alignment when the angle mismatch is small.

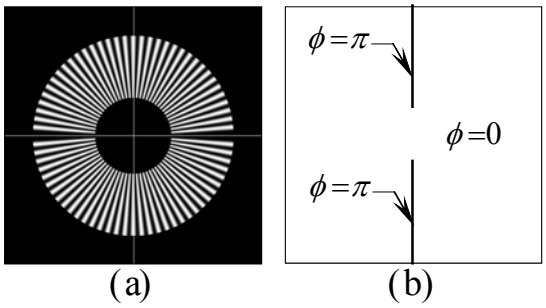

Figure 3.16. (a) Azimuth alignment test scene, and (b) filter.

The test filter consists of setting to π the phase difference between the background and those pixels along the y axis at a distance to the origin bigger than a given threshold. See Figure 3.16b. This filter produces the inversion of the sign of the diffraction orders along the y-axis (with a frequency higher than the threshold frequency). And therefore, this filter produces the contrast inversion of gratings that vary along the y axis with a frequency above the threshold, in the image reconstructed on the correlation plane.

To analyze the effect of the proposed filter on the scene it is necessary to find out its frequency content. Let us note that the wedge star in the scene can be approximated in each small region about a point by a linear grating whose direction and frequency are determined by the position of the point. Let us consider the wedges close to a point with polar coordinates(ρ,θ), their directions are in a small environment of θ. Therefore one can approximate the wedges by a linear grating whose bands are at that angle θ, what means that the variation direction of the grating is at $\theta+\pi/2$. In addition, the period of the linear grating

is given by the separation between two consecutive wedges. If we consider that the wedges are separated by an angle P, at the point (ρ,θ) they are separated by a linear period $P_L=\rho P$. In other words, the frequency of the local grating is $1/\rho P$. Taking all this into account, one can write the linear grating that approximates better the wedge star in a point (ρ,θ) as follows.

$$A_{\rho,\theta}(x,y)=\frac{A_0}{2}\left\{1+\cos\left[\frac{2\pi}{\rho P}(x\sin\theta-y\cos\theta)+\frac{\theta}{P}\right]\right\}, \qquad (3.17)$$

We represent in Figure 3.17 the approximation of the wedge star in the test scene by linear gratings considering square environments of different sizes. In Figure 3.17a the star is approximated in squares with side $N_x/6$. In each square we represent a linear grating with the frequency and orientation corresponding to its central pixel. Figure 3.17b and c represent the same approximation of the star, but in these cases we have used squares with sides $N_x/10$ and $N_x/16$ respectively. One can observe that Figure 3.17c is very approximate to the star of the azimuth test scene in Figure 3.16a.

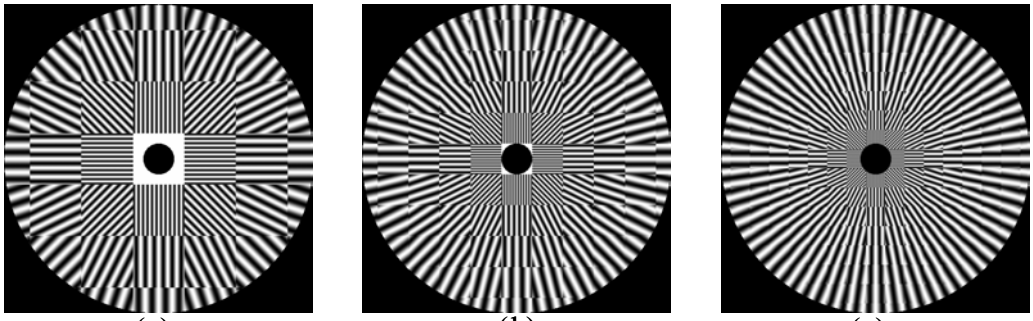

Figure 3.17. Approximation of the scene by linear gratings. The frequency and orientation of the grating is approximated at a square of side: (a) $N_x/6$,(b) $N_x/10$ and (c) $N_x/16$.

The azimuth test scene, and the magnitude of its Fourier spectrum are shown in Figure 3.18a and b, respectively. Because the frequency and orientation of the local gratings that compose the scene vary continuously, one does not observe discrete peaks in the Fourier spectrum, but a continuous distribution (see Figure 3.18b). It contains frequencies in all the directions because the wedges of the scene are directed in all the directions. The region of the scene located at a given direction θ from the origin, represented in Figure 3.18c, contains frequencies along the direction $\theta+\pi/2$ (see Figure 3.18d). In addition, the regions of the scene at a distance ρ from the origin (see Figure 3.18d) contribute with a frequency $1/\rho P$, as represented in Figure 3.18e.

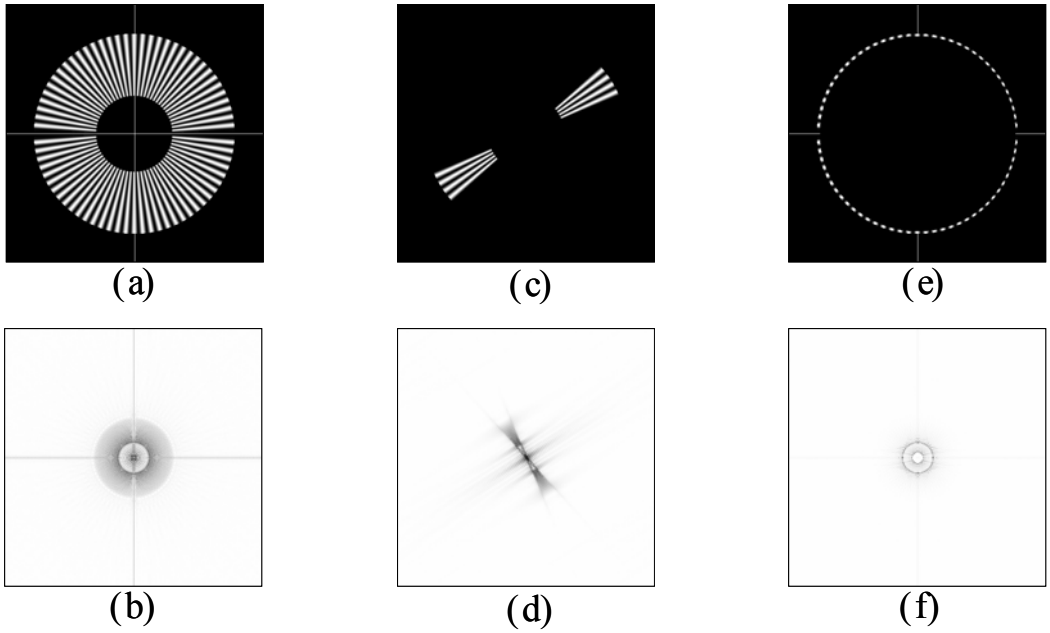

Figure 3.18. Frequency content of the test scene.(a) Test scene. (b) Fourier spectrum (c) Part of the scene along a given direction. (d) The corresponding frequencies are distributed along the orthogonal direction. (e) Part of the scene for a given radius (d) corresponding Fourier spectrum.

One can consider that the frequency filter proposed for the azimuth alignment test (see Figure 3.16b) inverts the sign of frequencies in the *y* direction defined by the filter SLM pixel array, but leaves unaltered the sign of the DC order. Therefore, in the reconstructed image of the scene at the correlation plane, the contrast of the gratings that contain that range of frequencies are inverted whatever it is a maximum intensity wedge (called ridge-wedge) or a minimum intensity wedge (called valley-wedge). If the orientation of the *x* axis of the filter SLM matches the direction of a wedge, one observes that a thin black line splits the wedge in two. If the *x* axis of the filter SLM is oriented between two wedges of the scene, a thin light line appears between the wedges. This way, one can measure in the

image reconstructed in the correlation plane the angle between the axes defined by the pixel arrays of the scene and the filter SLMs.

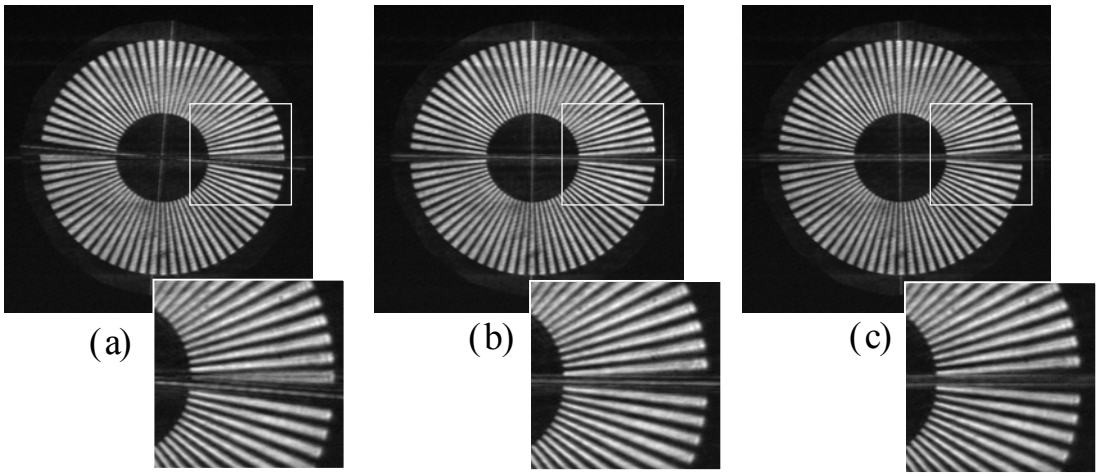

Figure 3.19. Experiments on the azimuth alignment. (a) Capture of the correlation plane for an azimuth mismatch of 5 degrees. (b) idem for 1 degree (c) idem for correct azimuth matching.

Experimental results obtained during the azimuth alignment of our correlator are shown in Figure 3.19. One can observe in Figure 3.19a that a thin black line appears on the first wedge. That indicates that the azimuth mismatch is 5 degrees. In Figure 3.19b we show that a thin line appears between the reference line and the first wedge when the azimuth difference is under five degrees (the figure corresponds to a mismatch of one degree). Finally, when the axes of the scene and the filter are aligned, the line whose contrast is inverted is the reference line on the *x* axis.(Figure 3.19c).

3.6.Filter scaling test

The last step of the alignment procedure of the correlator proposed in this Chapter is the scale matching between the Fourier scene spectrum and the filter. As mentioned in Section 3.2.2 this is done by displacing the scene SLM along the optical axis (*W* in Figure 3.2), and of course by refocusing the correlation plane.

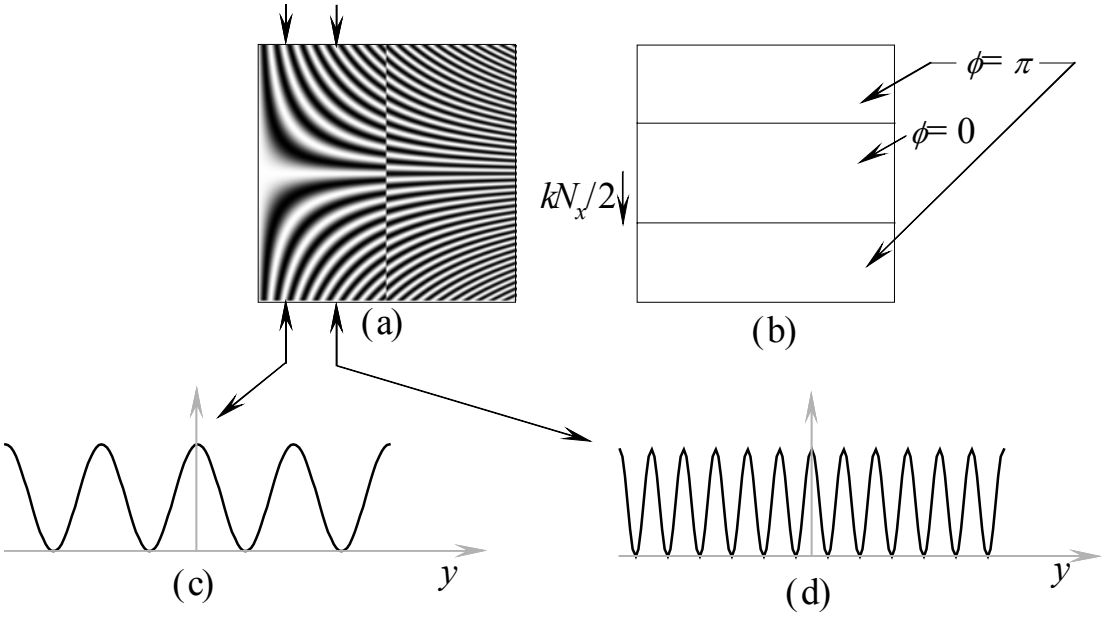

Figure 3.20. Scene and Filter for the scale matching test. (a) Test scene. (b) Test filter. (c) and (d) are the amplitude profiles corresponding to the two columns marked with arrows.

3.6.1. *Test scene and filter*

The test we propose to perform the scaling of the scene spectrum consists of displaying in the input SLM of the correlator the scene shown in Figure 3.20a. The proposed test filter is shown in Figure 3.20b.

The test scene can be interpreted as if each vertical line were a cosine grating, and the frequency of each one of these vertical gratings increased linearly along the x axis, being the zero frequency on the left edge of the image. We illustrate this in Figure 3.20c and d. There we have represented the amplitude profile of the images along two different columns. The profile in Figure 3.20d corresponds to a column at a distance to the left edge of the image that is three times the distance to the left edge of the column corresponding to Figure 3.20c. That means that the frequency of the grating in Figure 3.20d is three times bigger than the frequency of the grating in Figure 3.20c. In the scene, we have introduced an additional contrast inversion for the right half of the image. The inversion change is produced at x=0. The amplitude a(x,y) of the grating is then given by:

$$a(x,y)=\begin{cases}\frac{a_0}{2}\left[1+\cos k(x+N_x/2)y\right] & if \quad x\le 0\\ \frac{a_0}{2}\left[1-\cos k(x+N_x/2)y\right] & if \quad x>0\end{cases}, \qquad (3.18)$$

where k is a scaling factor that quantifies how fast the frequency of the gratings increases along the x axis, and N_x is the size of the image along the x direction. This way, the frequency for the grating corresponding to the x=0 axis is $kN_x/2$. We consider it as the threshold frequency for the test. So, in the test scene all the columns at the left half have frequencies below the threshold frequency, and at the right half the frequencies are above the threshold level.

The threshold frequency is also considered in the design of the test filter (shown in Figure 3.20b). It is given by:

$$H(x,y)=\begin{cases}\pi & if \quad y<-kN_x/2\\ 0 & if \quad |y|\le kN_x/2\\ \pi & if \quad y>kN_x/2\end{cases}, \tag{3.19}$$

That is, the filter is divided in three uniform regions, limited by the threshold frequency, and the phase difference between these regions is π radians. This way, the filter introduces a contrast inversion for all the frequencies whose y component is above the threshold frequency.

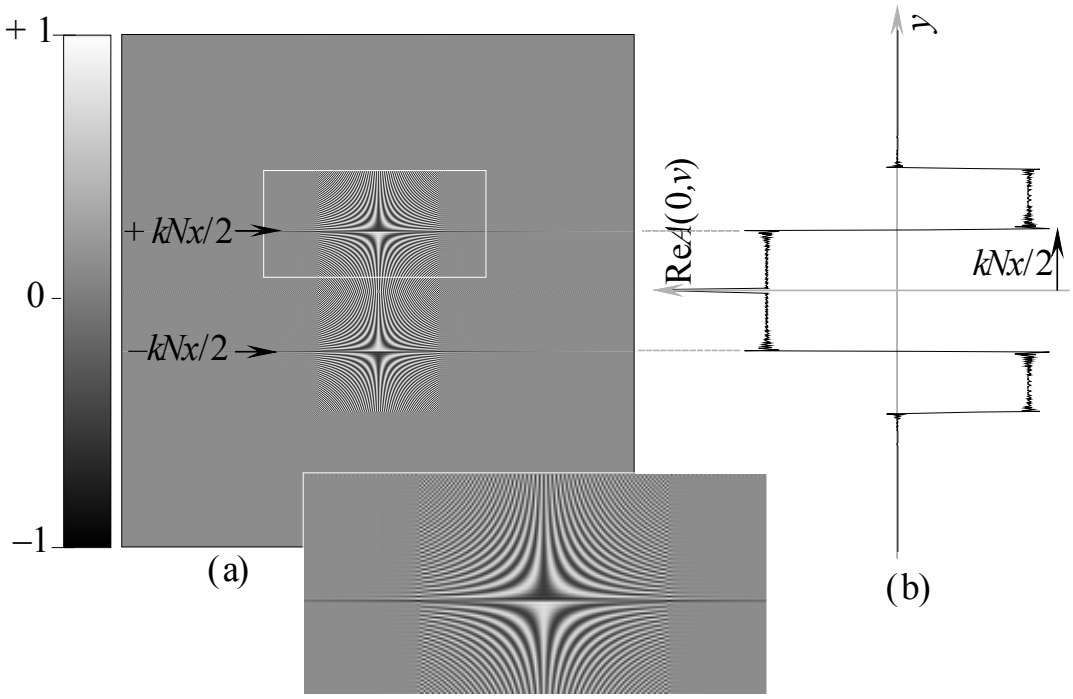

Figure 3.21. Spectrum of the scale matching test. (a) Real part of the Fourier spectrum. (b) Corresponding profile of the real part of the spectrum at the x=0 axis.

To show the effect of this filter in the reconstruction of the test scene we consider the frequency spectrum $A(x,y)$ of the scene. We show in Figure 3.21a the real part of the spectrum of the test scene. There, one can observe the discontinuities at the positive and negative orders of the threshold frequency ($+kN_x/2$ and $-kN_x/2$). These discontinuities come from the contrast inversion introduced in the scene.

Let us consider the frequency distribution of the spectrum along the x=0 axis. It corresponds to the addition of the one-dimensional spectra for all the columns of the scene. We represent the profile corresponding to its real part in Figure 3.21b. Because each column of the scene can be considered as an amplitude only cosine grating, it contributes to the frequency distribution along the x=0 axis with three real peaks, the DC term and the two fundamental orders. As the frequency in the scene is increased continuously along the x axis, the contribution of the peaks corresponding to each column of the scene constitute a continuous distribution in the Fourier spectrum. One can observe a discontinuity at the threshold frequency because the orders above the threshold frequency are negative while the orders below it are positive due to the contrast inversion introduced in the scene.

When the Fourier spectrum of the test scene is multiplied by the test filter, the sign of the orders above the threshold frequency is inverted, and therefore a contrast inversion of the corresponding gratings is produced. The contrast inversion

introduced by the filter, compensates the contrast inversion designed in the scene, only if the size between the filter and the diffraction pattern of the scene obtained in the correlator is the same.

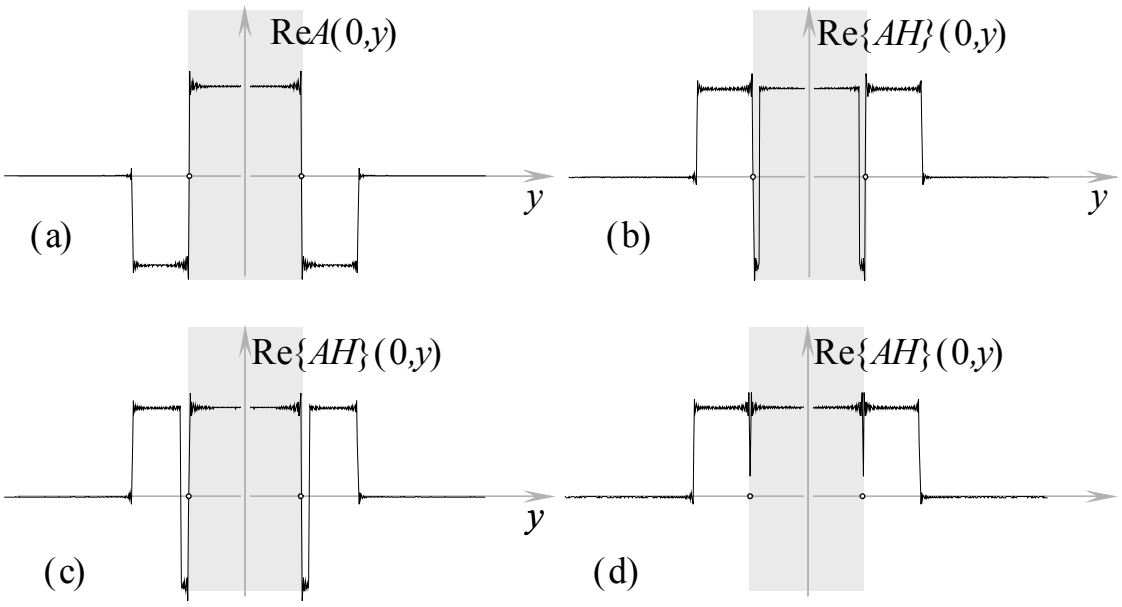

Figure 3.22. Inversion of the x=0 line of the spectrum for the filter scaling test. x=0 line of the spectrum (a) when it is not filtered, (b) when the filter is smaller than the scene spectrum, (c) when the filter is bigger than the scene spectrum., and (d) when the filter scale is matched.

If the scale is not matched, the contrast inversion introduced by the filter occurs at a different frequency to the contrast inversion designed in the scene. This is shown in Figure 3.22, the x=0 line of the Fourier spectrum of the test scene is represented for several scales of the test filter. In Figure 3.22a we represent the spectrum without filtering. In Figure 3.22b we represent the case in which the Fourier spectrum of the scene, obtained optically on the filter plane is bigger than the size assumed for the filter therefore one observes that the sign

inversion introduced by the filter occurs at a frequency below the threshold. The opposite case is represented in Figure 3.22c, there the filter is bigger than the Fourier spectrum of the scene and the contrast inversion introduced by the filter occurs for a frequency above the threshold frequency. Finally Figure 3.22d represents the case in which the scale of the filter is correctly matched. There one can observe that the sign of the filtered spectrum does not change along the x=0 axis.

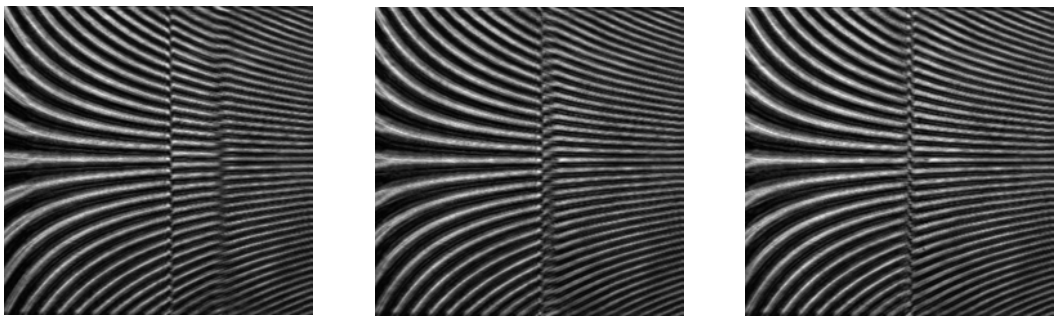

Figure 3.23. Experimental captures of the correlation plane for the scale matching test. (a) Image when the size of the filter is 1.5 times bigger than the proper size ,(b) when it is 1.01 bigger, and (c) when the scale is correctly matched.

In Figure 3.23 we show experimental captures of the correlation plane for different scales of the filter. Because the sign inversion of the orders in the spectrum produces a contrast inversion in the image retrieved in the correlation plane for the corresponding gratings, one can observe an additional contrast inversion in the correlation plane, besides the contrast inversion designed in the scene. These two contrast inversions compensate each other only in the case that the filter scale is correctly matched. Figure 3.23a shows the correlation plane

when the filter size is 1.5 times the size of the scene spectrum. One can observe that the contrast inversion introduced by the filter is produced in the right side of the image, that is, at a frequency higher than the threshold frequency. We show in Figure 3.23b the case in which the filter is 1.01 times bigger than the size of the scene spectrum. One can still differentiate that the contrast inversion introduced by the filter occurs at a frequency higher than the threshold. Finally, Figure 3.23c shows a capture of the correlation plane when the scene spectrum matches the size of the filter. In this case there is no contrast inversion because the filter compensates the contrast inversion designed in the original scene.

3.7. Alignment tests for phase encoded scene correlators

The proposed tests can also be adapted for its use in a phase encoded scene correlator, that is, correlators, in which the scene modulator (SLM_1) works in phase only regime. This way, the input image is encoded in a phase distribution. This phase distribution can be reconstructed as an intensity image in the correlation plane by applying a phase shift to the DC term of the frequency spectrum obtained in the filter plane. This technique is also used in Zernike's phase contrast microscopy (see for instance **[Zernike95]**).

Because the phase contrast is produced in the correlation plane when a phase shift is applied to the DC term of the Fourier

spectrum of the scene, obtained in the filter plane, the previous condition to perform any other operation involving phase contrast is to locate accurately the center of the Filter plane.

We remark that the filter focusing test is independent of the modulation regime of the test scene because it is performed with a uniform image in the scene. Therefore the explanation of this filter given in Section 3.3 is also valid for the phase-encoded scene correlator.

3.7.1. *Filter centering*

To perform the centering of the filter, a modification of the test presented in Section 3.4 is proposed so as to allow us its use in phase encoded scene correlators. It consists on displaying as scene the phase distribution shown in Figure 3.24a, and the filter in Figure 3.24b. The scene is a phase version of the amplitude encoded scene centering test scene but in this case the gratings take the values 1 (for ϕ=0) and i (for $\phi=\pi/2$). The filter consist on a line with a phase difference of $\pi/2$ rad to the background, along the y axis.

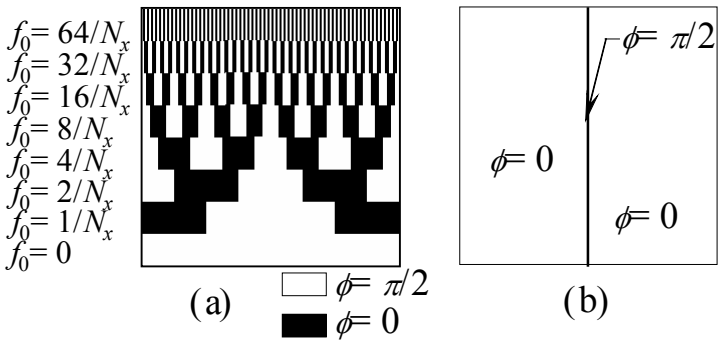

Figure 3.24. Phase only version of the filter centering test (a) Phase distribution of the scene. (b) Phase distribution of the filter.

The amplitude distribution of the scene in Figure 3.24a can be written as follows:

$$d(x) = \frac{A_{\max}}{\sqrt{2}} \exp i\frac{\pi}{4}\left(1 - i\,\mathrm{sgn}\cos 2\pi \frac{x}{x_0}\right), \qquad (3.20)$$

This expression is essentially the same expression as Equation 3.6 for the amplitude only grating described in Section 3.4.1. However, in this case the term independent of x presents a phase difference of $\pi/2$ radians to the remaining terms. In consequence, the frequency spectrum corresponding to such a grating presents the same peak distribution as for amplitude only case, but in this case the DC term is delayed by $\pi/2$ radians to the remaining terms.

We present in Figure 3.25a and b the amplitude distribution for the proposed binary phase grating and the corresponding frequency spectrum, respectively.

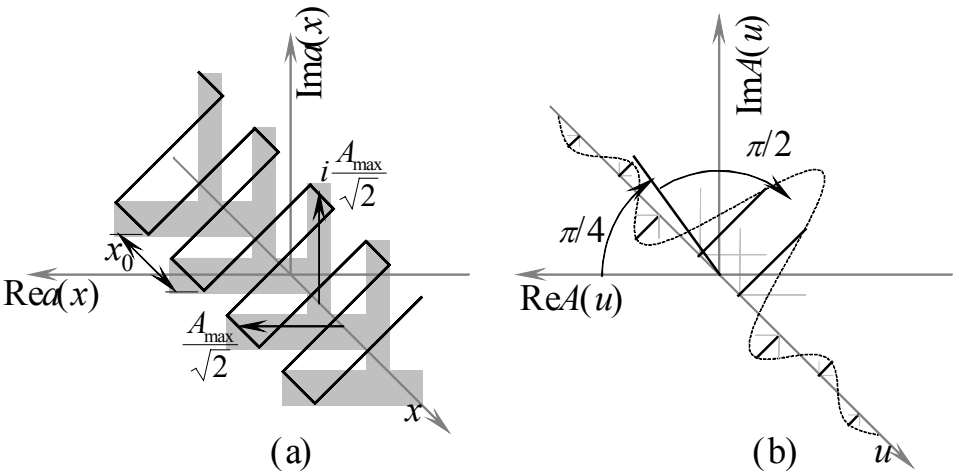

Figure 3.25. Binary phase only grating between zero and $\pi/2$ (a) Representation of the amplitude in the complex plane as a function of x (b) Representation of the corresponding Fourier spectrum.

It is trivial to demonstrate that this amplitude distribution corresponds to a uniform intensity distribution. However this is true only if the infinite orders of the Fourier series are considered, so if we consider a limited number of terms, the edges of the grating are not perfectly squared, and then the edges are contrasted. This is the case of the optical correlator, because its elements have limited aperture and they remove some of the diffraction orders of the gratings in the scene. In Figure 3.26 we show an experimental capture of the correlation plane when the phase only scene in Figure 3.24a is represented in the input plane of the correlator and a uniform filter is presented in the SLM_2. One can observe that the edges of the gratings are visible due to the vignetting on the correlator.

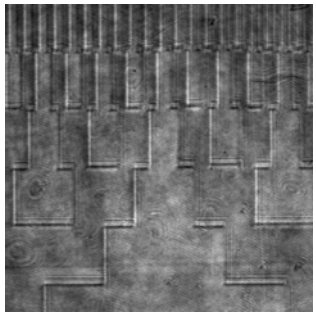

Figure 3.26. Image at the correlation plane of phase only scene of the filter centering test.

For the phase encoded scene, the test filter consists of a line that coincides with the y axis and that has $\pi/2$ radians of phase shift with respect to the background, it is represented in Figure 3.24b. When the line on the filter overlaps one of the diffraction orders of a single grating, it delays its phase by $\pi/2$ radians, and therefore, the corresponding cosine term is changed. The effect of this filter, noted $H[]$, is given by next expression:

$$H[\cos(x)] = \exp i\tfrac{\pi}{4}\cos(x+\tfrac{\pi}{4}), \qquad (3.21)$$

Therefore, when the n-th diffraction order of one of the gratings is affected, the amplitude at the correlation plane, $a_C(x)$, can be written as a function of the original amplitude distribution in the input plane $a(x)$ (equation 3.20) plus an increment function $b(x)$, let us say:

$$a_C(x) = a(x) + b(x). \qquad (3.22)$$

The increment function $b(x)$ is given by:

$$b(x) = \frac{A_n}{\sqrt{2}}\left[\exp i\tfrac{\pi}{4}\cos 2\pi\frac{nx}{x_0} + \cos\left(2\pi\frac{nx}{x_0}+\frac{\pi}{4}\right)\right], \qquad (3.23)$$

In this case the intensity at the correlation plane is given by:

$$I_C(x) = I_S + b^2(x) - 2|a(x)b(x)|\cos[\arg a(x) - \arg b(x)], \qquad (3.24)$$

what is not a uniform intensity distribution. That means that the reconstruction of the grating presents a non uniform intensity distribution when one of its Fourier orders is affected by the filter, and in consequence it becomes visible in the correlation plane. The alteration of the grating is proportional to A_n^2, that is to the intensity of the peak affected by the phase line in the filter. In practice that means that the effect is mainly visible when the fundamental order of the grating is affected.

This way, as we did in Section 3.4, the filter allows to evaluate the real position of the filter by observing in the correlation plane which grating is affected. When the phase line crosses the origin of the scene spectrum, the phase delay between the DC order and the other diffraction orders of the gratings in the scene is compensated. Therefore the entire image suddenly becomes visible in the correlation plane

This is illustrated in Figure 3.27. We represent experimental captures of the correlation plane obtained using the described test for different positions of the filter SLM. Figure 3.27a and b show the intensity distribution of the reconstructed image when the filter is misaligned by eight and four pixels respectively. One observes that only one of the gratings is affected at each image. The higher the period of the affected grating, the closer to the correct position the filter is. Figure 3.27c shows the correlation

plane when the filter reaches the correct position. One can observe that all the gratings of the scene appear with very good contrast.

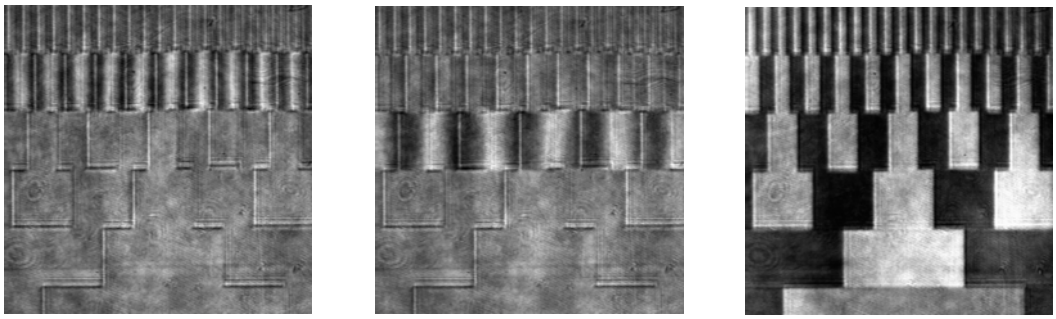

Figure 3.27. Filter centering test results. (a) Capture of the crrelation plane for a misalignment of 8 pixels, (b) idem for a misalignment of 4 pixels (c) Capture of the correlation plane when the filter is centered.

3.7.2. *Azimuth filter*

Note that once the center of the filter is correctly aligned, the phase delay of the DC with respect to the other orders can be compensated. When this phase difference is compensated, the resulting spectrum of the binary grating of values 0 and $\pi/2$ is identical to the spectrum of the amplitude only grating, except by a global phase. Applying this, one can adapt the remaining tests to the phase encoded scene correlator by simply compensating the $\pi/2$ phase delay in the DC term for the phase only gratings, and by considering the versions for the amplitude encoded scene correlator.

This way, the scene for the azimuth alignment test is the scene presented in Figure 3.28a, that takes the two phase values 0 and

$\pi/2$. Also in this case the wedge star can be approximated locally by linear gratings, as in section 3.5. However, in this case, the linear gratings are binary phase gratings of values 0 and $\pi/2$, what involves that the DC term is delayed by $\pi/2$ radians to the other terms.

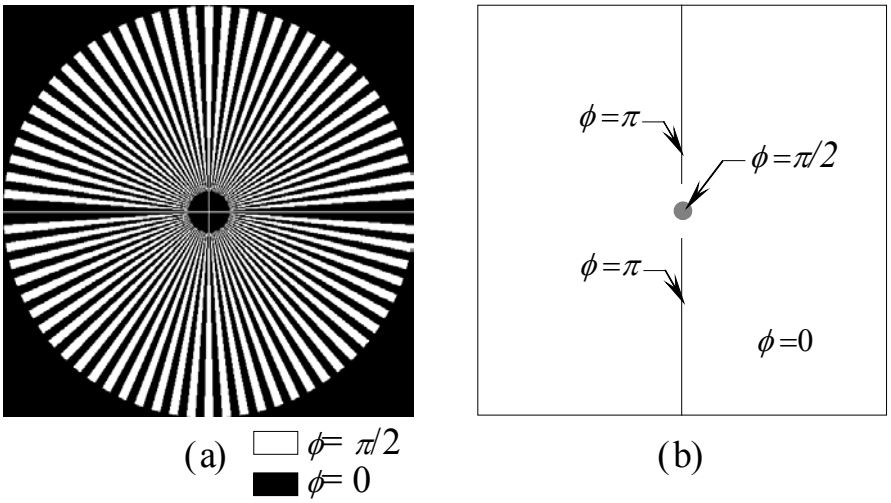

Figure 3.28. Azimuth test for phase-only scene correlator. (a) Test scene (b) Test filter.

According to that, a modification is introduced in the test filter, shown in Figure 3.28b. Aside from the segments on the x=0 axis with a phase difference of π to the background, the central pixels of the filter are set to a phase of $\pi/2$ radians with respect to the background. So, the delay of the DC term of the scene Fourier spectrum is compensated and the phase only scene is contrasted in the correlation plane. Once the filtered scene is contrasted in the correlation plane, the azimuth alignment is carried out by observing the wedge splitting effect produced by the π phase line on the x=0 axis of the filter, as the case for the amplitude only scene.

We show the experimental results for this test in Figure 3.29. The correlation plane for a misalignment of 5 degrees is shown in Figure 3.29a. One can observe that the first wedge is split in two by a dark line in its center. Figure 3.29c shows the intensity distribution at the correlation plane when the azimuth is correctly aligned, in this case one can observe that the reference line is split in two by a dark line in its center. .

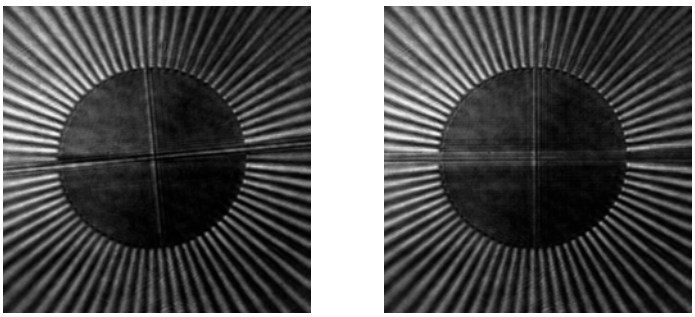

(a) (b)

Figure 3.29. Azimuth alignment test for phase only scene correlator (a) correlation plane for a misalignment of 5 degrees. (b) idem for correct azimuth alignment.

3.7.3. *Scale matching*

The same principle is applied to design a version of the scale matching test for phase only scene correlators. The test scene (Figure 3.30a) is very similar to the test scene shown in Section 3.6, but now it takes the two phase only values zero and $\pi/2$. Also in this case, we can consider that each column in the scene is a binary phase grating with frequency that increases linearly along the x axis. As we showed in Section 3.7.1, this binary phase only grating has the same Fourier spectrum as the

amplitude only version, except for the DC term, that in this case is delayed by $\pi/2$ with respect to the remaining orders.

Therefore, we introduce an additional spot in the center of the filter so as to compensate the phase delay of the DC term. The resulting filter is shown in Figure 3.30b. As in the case of the amplitude only scaling test, it contains three regions, limited at the threshold frequency where the contrast inversion is designed in the scene. The top and lower regions have a phase difference of π radians to the center background, and the spot in the center has a phase difference of $\pi/2$ radians. This way, the phase only distribution in the scene plane is contrasted onto an intensity distribution in the correlation plane.

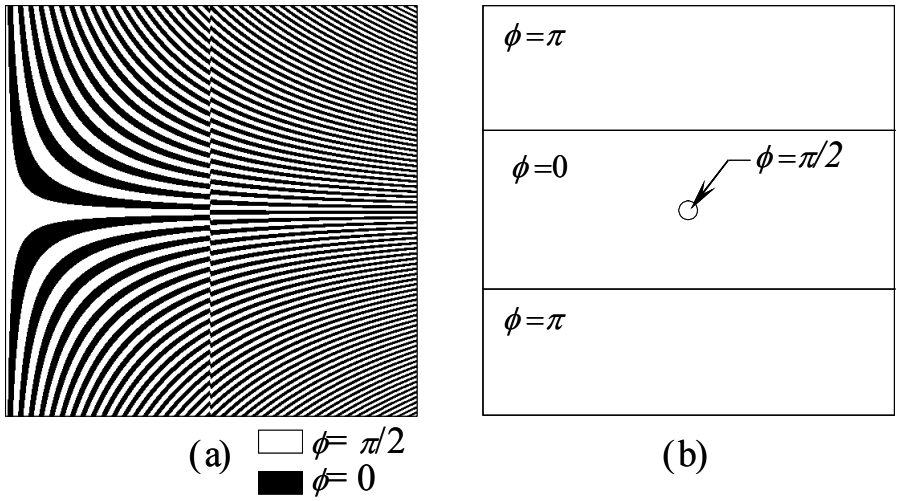

Figure 3.30. Phase only scene scaling test. (a) Test scene. (b) Test filter.

Once the phase delay of the DC term is compensated, the Fourier spectrum for this scene is equal to the amplitude only version of the test. Therefore, the test works in the same way as in section 3.6. The frequencies above the threshold frequency

are delayed by π radians, what involves a contrast inversion in one side of the reconstruction of the scene. The frequency where this contrast inversion is produced indicates the scale of the Fourier spectrum of the scene with respect to the size of the filter encoded in SLM_2.

We show in Figure 3.31 experimental captures of the correlation plane when this test is being used for the scale matching. We show in Figure 3.31a the correlation plane when the scale mismatch is a 1%, that is, when the size of the filter is 1.01 times the size of the Fourier spectrum of the scene. One can observe that the phase only distribution of the test scene (SLM_1) is contrasted in the correlation plane. One can also observe that the test filter introduces a contrast inversion at a frequency bigger than the reference one. In the case when the scale is properly matched the contrast inversion introduced by the filter is produced at the threshold frequency, this way it compensates the contrast inversion introduced in the design of the scene. This is shown in Figure 3.31b.

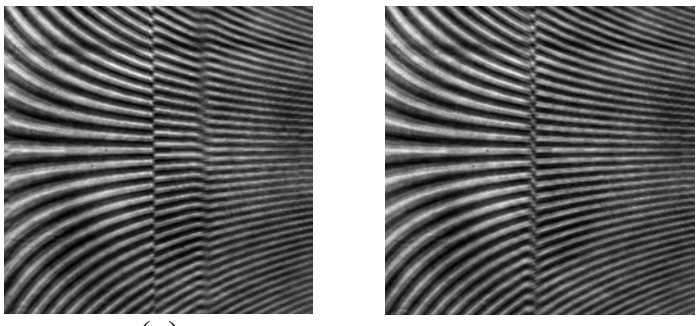

(a) (b)

Figure 3.31 Experimental results for phase only scene scaling test. (a) Correlation plane for a mismatch of 1%. (b) Correlation plane for correct scaling of the filter.

3.8.Summary

A procedure based on simple scene and filter tests are proposed in this Chapter to perform the alignment of an optical convergent correlator for either amplitude or phase encoded scenes. All the alignment sequence is based in the observation of the reconstructed image of the scene in the correlation plane and the interpretation of the effects of the filtering.

The proposed tests constitute a series of objective criteria for the alignment of the correlator, in the sense that experimental observations are interpreted in accordance to a simple frequency filtering theory.

For all the tests we have presented experimental results that demonstrate the correct alignment of the filter or the scene SLMs.

In conclusion we have shown that the proposed tests constitute a good method to solve the main drawback (the alignment requirements) of the Vander Lugt based correlator.